Unstable dimension variability and heterodimensional cycles in the border-collision normal form

Document Version
Accepted author manuscript

Published in:
Physical Review E: covering statistical, nonlinear, biological, and soft matter physics

Unstable dimension variability and heterodimensional cycles in the border-collision normal form.

P.A. Glendinning

Department of Mathematics, University of Manchester, Manchester, M13 9PL UK

D.J.W. Simpson

School of Mathematical and Computational Sciences,
Massey University, Palmerston North, 4442, New Zealand

(Dated: July 9, 2023)

Chaotic attractors commonly contain periodic solutions with unstable manifolds of different dimensions. This allows for a zoo of dynamical phenomena not possible for hyperbolic attractors. The purpose of this Letter is to emphasise the existence of these phenomena in the border-collision normal form. This is a continuous, piecewise-linear family of maps that is physically relevant as it captures the dynamics created in border-collision bifurcations in diverse applications. Since the maps are piecewise-linear they are relatively amenable to an exact analysis. We explicitly identify parameter values for heterodimensional cycles and argue that the existence of heterodimensional cycles between two given saddles can be dense in parameter space. We numerically identify key bifurcations associated with unstable dimension variability by studying a one-parameter subfamily that transitions continuously from where periodic solutions are all saddles to where they are all repellers. This is facilitated by fast and accurate computations of periodic solutions; indeed the piecewise-linear form should provide a useful test-bed for further study.

1. DIFFERING DIMENSIONS OF INSTABILITY

Chaotic attractors of one-dimensional non-invertible maps and two-dimensional invertible maps have one unstable direction locally. For higher dimensional maps the dimensions of the unstable manifolds of periodic orbits within a chaotic attractor can differ, and this can occur also for ODEs. This phenomenon is known as *unstable dimension variability* (UDV). It generates non-hyperbolic dynamics [1] and is expected to be common for chaotic attractors in mathematical models with sufficiently many variables [2–4]. UDV implies the existence of orbits that spend arbitrarily long times close to an unstable manifold of one dimension, and arbitrarily long times close to an unstable manifold of another dimension [5]. It follows that finite-time Lyapunov exponents fluctuate about zero as the system evolves [6, 7]. It further follows that numerical solutions may differ wildly from actual orbits. This lack of 'shadowing' is problematic for the applicability of mathematical models [8, 9].

One mechanism that implies UDV is the existence of a *heterodimensional cycle* — a heteroclinic connection between saddle objects with unstable manifolds of different dimensions. If an attractor contains a heterodimensional cycle, then it has UDV [10]. A given heterodimensional cycle is at least codimension-one, and recent advances in numerical methods have led to the identification of heterodimensional cycles in an ODE model of intracellular calcium dynamics [11, 12].

Constructions of robust non-hyperbolic chaotic invariant sets in diffeomorphisms often use the idea of a *blender* [1, 13]. These are transitive hyperbolic sets whose stable manifold acts geometrically (in terms of its intersections with other manifolds) as an object with dimension greater than the stable index of the hyperbolic set, and for which this property persists for all sufficiently close diffeomorphisms [10, 14]. Blenders can be used to construct heterodimensional cycles by providing robust intersections between stable and unstable manifolds [15, 16], and have recently been identified numerically [17, 18].

This paper treats maps that are neither invertible nor C^1 so the formal definition of a blender, including its persistence property, do not directly apply. Previous works have considered specific piecewise-linear maps [19]; in this Letter we demonstrate the prevalence of differing dimensions of instability in a normal form. For invertible maps the above notions require at three dimensions [20–22]; for non-invertible maps (Sections 3 and 4) two dimensions are sufficient [23].

2. THE BORDER-COLLISION NORMAL FORM

Border-collision bifurcations (BCBs) occur when a fixed point of a piecewise-smooth map collides with a boundary (switching manifold) where the functional form of the map changes. They have been identified as the onset of chaos and other dynamics in applications including power electronics [24], mechanical systems with stick-slip friction [25, 26], and economics [27]. Near a BCB the dynamics are well-approximated by a piecewise-linear map [28]. The border-collision normal form (BCNF) then results from a change of coordinates [29, 30]. In two dimensions this form is

$$x \mapsto \begin{cases} A_L x + b, & x_1 \leq 0, \\ A_R x + b, & x_1 \geq 0, \end{cases} \tag{1}$$
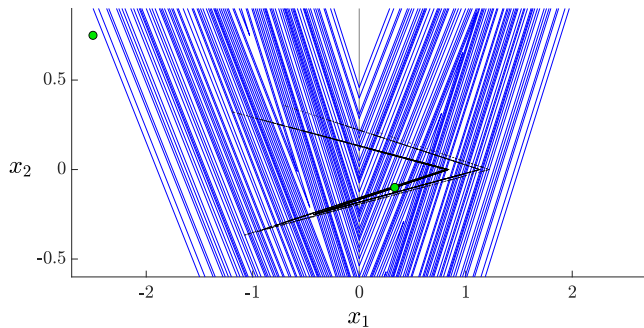
FIG. 1. A phase portrait of an invertible instance of the two-dimensional BCNF (1)–(2); specifically $(\tau_L, \delta_L, \tau_R, \delta_R) = (1.7, 0.3, -1.7, 0.3)$. In black we show 8000 consecutive iterates of a typical forward orbit with transients removed (this represents the attractor of the map). The green circles are fixed points; the blue lines show the stable manifold (grown outwards numerically some amount) of the right-most fixed point.

where

$$A_L = \begin{bmatrix} \tau_L & 1 \\ -\delta_L & 0 \end{bmatrix}, \quad A_R = \begin{bmatrix} \tau_R & 1 \\ -\delta_R & 0 \end{bmatrix}, \quad b = \begin{bmatrix} 1 \\ 0 \end{bmatrix}, \quad (2)$$

and $x = (x_1, x_2) \in \mathbb{R}^2$. Here $\tau_L, \delta_L, \tau_R, \delta_R \in \mathbb{R}$ are parameters; the BCB parameter, usually denoted μ, has been scaled to 1.

The dynamics and bifurcation structure of (1)–(2) is incredibly rich [31–33]. It exhibits robust chaos [34] in the sense that chaotic attractors exist throughout open regions of (four-dimensional) parameter space, even with $\delta_L \delta_R > 0$ where the map is invertible. Fig. 1 shows a phase portrait of such an attractor. The attractor contains a saddle fixed point whose stable manifold is dense in an open region of phase space. This denseness property holds throughout an open region of parameter space, proved in [35] via a series of geometric arguments by bounding the rate at which line segments expand. A similar result was obtained earlier by Misiurewicz [36] for the Lozi family (the special case $\tau_L = -\tau_R$ and $\delta_L = \delta_R$).

We believe the chaotic attractor and denseness of the stable manifold is robust to C^1 perturbations to the pieces of (1). This is because piecewise-smooth maps lack smooth turning points where derivatives vanish, and indeed we proved a result of this type in [37]. Also, stable periodic solutions are typically absent near structurally unstable homoclinic connections [38].

3. TRANSITION THROUGH UNSTABLE DIMENSION VARIABILITY

The parameter space of the two-dimensional BCNF has regions where the map has a chaotic attractor in which (the dense set of) periodic solutions are all saddles, and other regions where the map has a chaotic attractor

in which periodic solutions are all repellers. In this section we interpolate between two such regions and provide numerical evidence for robust UDV.

Let $x \in \mathbb{R}^2$ be a period-n point of (1)–(2) and suppose its forward orbit does not intersect the switching manifold (as is generically the case). Each point in the orbit has a neighbourhood in which the map is differentiable (in fact affine). Thus it has two stability multipliers, and if neither of these has modulus 1, the orbit is hyperbolic. In this case let $k \in \{0, 1, 2\}$ denote the number of stability multipliers with modulus greater than 1 (k is the unstable index). Then x is asymptotically stable if $k = 0$, a saddle if $k = 1$, and a repeller if $k = 2$.

We now explore a one-parameter family of examples. In (2) we use

$$\begin{aligned}
\tau_L &= (1-a)\tau_{L,0} + a\tau_{L,1}, \\
\delta_L &= (1-a)\delta_{L,0} + a\delta_{L,1}, \\
\tau_R &= (1-a)\tau_{R,0} + a\tau_{R,1}, \\
\delta_R &= (1-a)\delta_{R,0} + a\delta_{R,1},
\end{aligned} \quad (3)$$

with $0 \le a \le 1$ and

$$\begin{aligned}
\tau_{L,0} &= 0.8, & \tau_{L,1} &= 0.8, \\
\delta_{L,0} &= -0.8, & \delta_{L,1} &= -1.2, \\
\tau_{R,0} &= -2.8, & \tau_{R,1} &= -1, \\
\delta_{R,0} &= 0.8, & \delta_{R,1} &= 2.4.
\end{aligned} \quad (4)$$

This one-parameter family has been chosen for three reasons. First, with $a = 0$ all periodic solutions are saddles, Fig. 2-a. This is because with $|\delta_L|, |\delta_R| < 1$ both pieces of (1) are area-contracting so repellers are not possible, while stable periodic solutions are not possible because an invariant expanding cone can be constructed in tangent space [39]. Second, with $a = 1$ all periodic solutions, except the left-most fixed point, appear to be repellers, Fig. 2-c. This has been proved for nearby parameter combinations where there exists a simple Markov partition [40, 41]. Third, the map appears to have a unique attractor for all $0 \le a \le 1$. The two Lyapunov exponents of the attractor are shown in Fig. 3. These were computed numerically using the standard QR-factorisation method [42, 43].

For any $0 \le a \le 1$, let $\mathcal{N}(k, n; a)$ denote the number of period-n points that have k stability multipliers with modulus greater than 1. The sum of these numbers up to $n = 25$ is plotted in Fig. 4-a. This figure was computed by brute-force. We used Duval's algorithm [44, 45] to generate all sequences of L's and R's of length $n \le 25$. Interpreting these as applications of (1) on the left or on the right respectively, the (generically) unique point that has period n in the order specified by each sequence was identified for each value of a [28]. We then checked by iterating the map whether the order of the images of the point matched the order of the specified sequence (an *admissibility* condition). For those admissible sequences the stability multipliers were evaluated to determine whether the periodic solution is a saddle or a repeller.
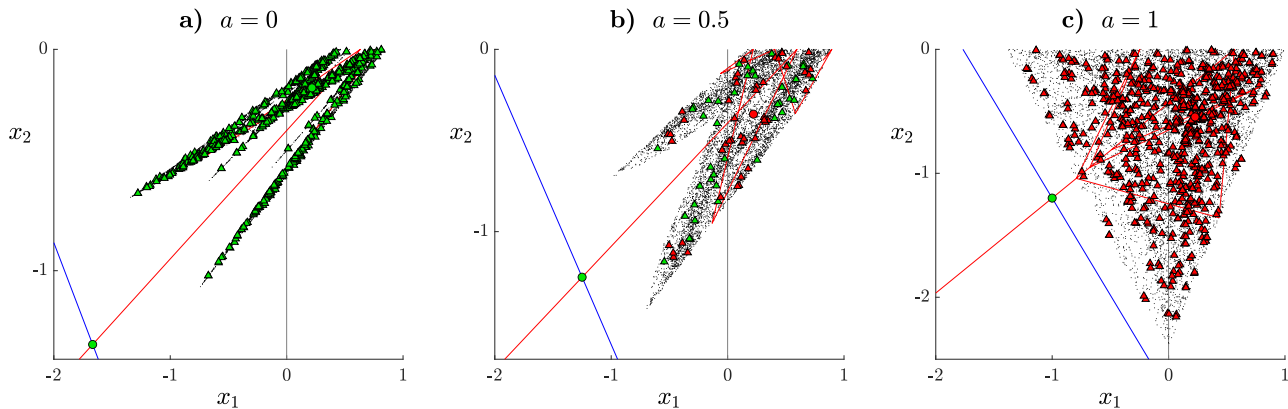
FIG. 2. Phase portraits of non-invertible instances of the two-dimensional BCNF (1)–(2). The parameter values are given by (3) with (4) and three different values of a. The black dots show iterates of a typical forward orbit with transients removed. Periodic points (up to period 10) are shown with triangles, except fixed points are shown with circles. Saddles are coloured green; repellers are coloured red. The stable (blue) and unstable (red) manifolds of the left-most fixed point are also shown (grown outwards a small amount).
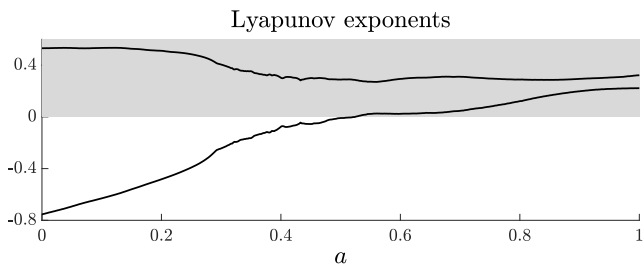

FIG. 3. Numerically computed Lyapunov exponents of the attractor of (1)–(2) with (3) and (4).
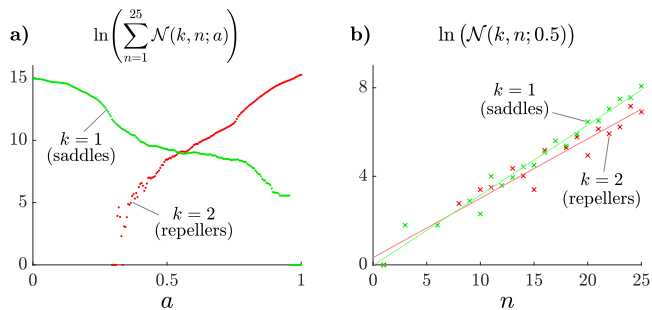

FIG. 4. Plots involving $\mathcal{N}(k, n; a)$: the number of period-n points (saddles for $k = 1$; repellers for $k = 2$) of (1)–(2) with (3) and (4). Panel (b) includes lines of best fit.

For an intermediate range of values of a, the attractor contains both saddles and repellers, thus exhibits UDV. The point of cross-over, where saddles and repellers exist in the same proportion, is close to $a = 0.5$ and matches well to where the lower Lyapunov exponent becomes positive. Fig. 2-b shows a phase portrait with $a = 0.5$; Fig. 4-b shows that here the number of saddles and repellers appears to increase exponentially with n. This suggests

that saddles and repellers are both dense in the attractor.

Saddles and repellers can arise in different ways. As the value of a is decreased from 1, saddles are created in a BCB of two saddle period-five solutions at $a \approx 0.9592$. Here infinitely many saddle periodic points are created because the BCB also creates robust heteroclinic connections between the period-five solutions. This appears to be where saddles are first created and explains the large discontinuity in the number of saddle points in Fig. 4-a. In contrast, as the value of a is increased from 0, repellers are created and destroyed in many bifurcations. For example a saddle period-nine solution (with only one point in $x_1 < 0$) becomes repelling at $a \approx 0.3278$ when one of its stability multipliers decreases through -1, then is destroyed in a BCB at $a \approx 0.3321$.

Since the maps are non-invertible, repelling sets may have preimages, i.e. they may have zero-dimensional stable manifolds leading to phenomena such as snap-back repellers [46]. Such a stable manifold may intersect an unstable manifold of a saddle resulting in a heterodimensional cycle, assuming their other invariant manifolds intersect as can be expected. We conjecture that the BCB at $a \approx 0.9592$ is the boundary for the existence of heterodimensional cycles in our example. This is because the unstable manifold of the saddle chaotic set associated with the period-five heteroclinic connection and the stable manifolds of the innumerable repellers should be sufficiently voluminous to intersect for a dense set of values of a. The analogous transition at lower values of a is less clear. It may be that 'enough' repellers are needed before heterodimensional cycles can occur for dense set of values of a, or possibly over an interval.
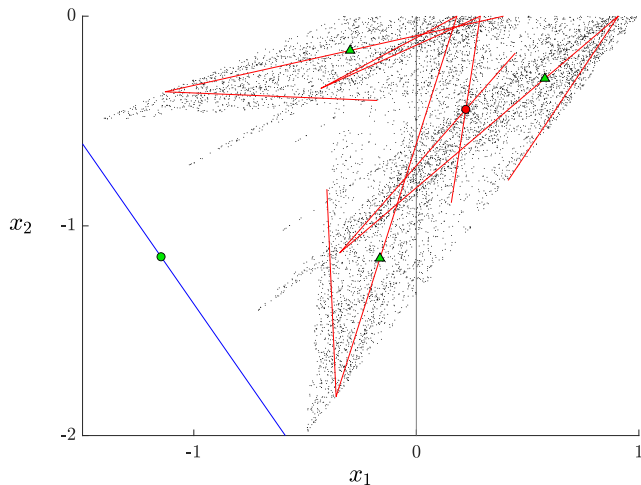
FIG. 5. A phase portrait of a non-invertible instance of the two-dimensional BCNF, (1)–(2) with (5). The black dots show iterates of a typical forward orbit with transients removed. The blue line is the initial part of the stable manifold of the left-most fixed point (green circle). The red lines show part of the unstable manifold of a period-three solution (green triangles). The value of τ_L has been chosen so that this manifold intersects the right-most fixed point (red circle).

4.   AN EXPLICIT HETERODIMENSIONAL CYCLE

We now provide a simple example of a heterodimensional cycle. Fig. 5 shows a phase portrait of (1) with

$$\tau_L \approx 0.8716, \quad \delta_L = -1, \quad \tau_R = -1.5, \quad \delta_R = 2, \quad (5)$$

where the exact value of τ_L will be clarified in a moment. With these values the right-most fixed point (red circle), call it x^R, is repelling. There also exists a saddle period-three solution (green triangles). The value of τ_L has been chosen so that the unstable manifold of the period-three solution intersects x^R. By using computer algebra to analytically find where a certain fourth preimage of x^R lies on the initial linear part of the unstable manifold, we found that τ_L is a root of

$$108\tau_L^6 + 495\tau_L^5 + 258\tau_L^4 + 1184\tau_L^3 - 5800\tau_L^2 - 4907\tau_L + 7454. \quad (6)$$

The (two-dimensional) unstable manifold of x^R appears to intersect the stable manifold of the period-three solution (as one would expect), thus these orbits have a heteroclinic connection. This is a heterodimensional cycle because x^R and the period-three solution have unstable manifolds of different dimensions. This cycle is codimension-one because their dimensions differ by one; indeed the cycle was obtained by carefully adjusting the value of one parameter (namely τ_L).

Fig. 5 is the simplest example of a heterodimensional cycle that we have found for (1)–(2) where the cycle is contained in an attractor. This suggests that, as in Fig. 2-b, the attractor exhibits UDV.

5.   UNSTABLE DIMENSION VARIABILITY IN INVERTIBLE MAPS

For an invertible map to have a heterodimensional cycle, the map needs to be at least three dimensional. This can also be demonstrated with the BCNF. In three dimensions the BCNF is (1) with

$$A_L = \begin{bmatrix} \tau_L & 1 & 0 \\ -\sigma_L & 0 & 1 \\ \delta_L & 0 & 0 \end{bmatrix}, \quad A_R = \begin{bmatrix} \tau_R & 1 & 0 \\ -\sigma_R & 0 & 1 \\ \delta_R & 0 & 0 \end{bmatrix}, \quad b = \begin{bmatrix} 1 \\ 0 \\ 0 \end{bmatrix}, \quad (7)$$

and $x = (x_1, x_2, x_3) \in \mathbb{R}^3$, and has been studied previously for instance in [47, 48].

Fig. 6 shows a phase portrait using

$$\tau_L = 0.7228540306, \quad \sigma_L = -1, \quad \delta_L = -0.2,$$
$$\tau_R = -1.5, \qquad\qquad \sigma_R = 2, \quad\;\; \delta_R = -0.2. \quad (8)$$

These values were obtained by adding a dimension to the example of Fig. 5, varying δ_L and δ_R from 0 to create fully three-dimensional dynamics, and lastly adjusting the value of τ_L (to 10 decimal places) so that the one-dimensional unstable manifold of the period-three solution approximately intersects the one-dimensional stable manifold of x^R. The pink square in Fig. 6 shows this approximate point of intersection. Since the invariant manifolds appear to be embedded in an attractor, the other invariant manifolds presumably intersect forming a heterodimensional cycle. Hence this attractor too has UDV.

Numerically we have grown the unstable manifold of the period-three solution outwards much further than that shown in Fig. 6. Fig. 7 shows the intersections of this manifold with the switching manifold $x_1 = 0$ and reveals a quasi-one-dimensional structure. We have observed this structure appears to persist as parameters are varied and for different cross-sections. This suggests that the unstable manifold intersects a given one-dimensional stable manifold for a dense set of parameter values. That is, heterodimensional-cycles between two given saddles can be expected to occur on dense subsets of parameter space.

6.   DISCUSSION

The existence of UDV due to blenders has been established numerically in three-dimensional generalisations of the Hénon map [2]. We have considered a related piecewise-linear family and by interpolating between parameters with only saddles and parameters with only repellers we have provided strong numerical evidence for the existence of UDV in the two-dimensional non-invertible BCNF and the three-dimensional invertible BCNF. Since the BCNF describes BCBs in general piecewise-smooth systems, the existence of UDV in
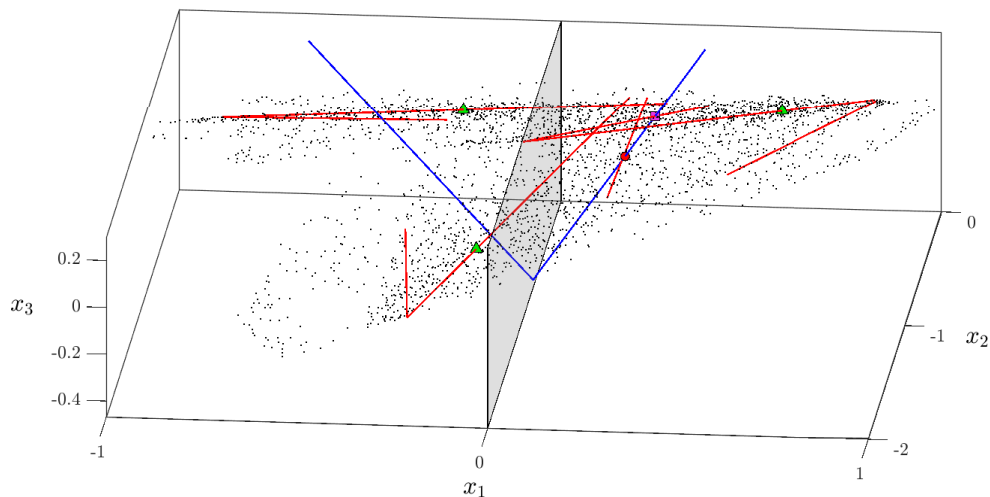
FIG. 6. A phase portrait of an invertible instance of the three-dimensional BCNF, (1) with (7) and (8). The black dots show iterates of a typical forward orbit with transients removed. The one-dimensional stable manifold of a fixed point (red circle) approximately intersects the one-dimensional unstable manifold of a period-three solution (green triangles). One point of intersection is indicated with a pink square.
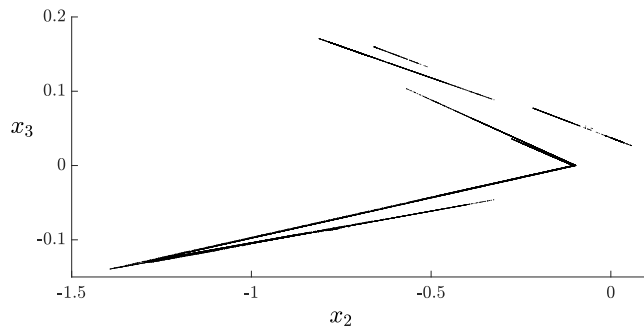

FIG. 7. Intersections of the one-dimensional unstable manifold of the period-three solution of Fig. 6 with $x_1 = 0$. This was computed by growing the manifold much further than that shown in Fig. 6.

these examples shows that UDV has broader significance within the study of piecewise-smooth dynamical systems and their applications.

We have also identified a possible mechanism for the onset of UDV through the creation of saddle chaotic sets (as the parameter a in Fig. 4 decreases) and snap-back repellers (as a increases). It is possible that bifurcation theory approaches [49, 50] are sufficient to prove persistent UDV without persistent HD-cycles in these examples. On the other hand the bifurcations may provide stable and unstable manifolds of the appropriate dimensions and complexity to create dense sets of parameter values with heterodimensional-cycles. This is weaker than the robustness provided by a blender, but much simpler and possibly sufficient for persistent UDV.

ACKNOWLEDGEMENTS

References

[1] C. Bonatti and L.J. Díaz. Persistent nonhyperbolic transitive diffeomorphisms. *Ann. Math.*, 143(2):357–396, 1996.

[2] Y. Saiki, M.A.F. Sanjuán, and J.A. Yorke. Low-dimensional paradigms for high-dimensional hetero-chaos. *Chaos*, 28(10):103110, 2018.

[3] R.L. Viana and C. Grebogi. Unstable dimension variability and synchronization of chaotic systems. *Phys. Rev. E*, 62(1):462–468, 2000.

[4] S. Das and J.A. Yorke. Multichaos from quasiperiodicity. *SIAM J. Appl. Dyn. Syst.*, 16(4), 2017.

[5] E.J. Kostelich, I. Kan, C. Grebogi, E. Ott, and J.A. Yorke. Unstable dimension variability: A source of non-hyperbolicity in chaotic systems. *Phys. D*, 109:81–90, 1997.

[6] S. Dawson, C. Grebogi, T. Sauer, and J.A. Yorke. Obstructions to shadowing when a Lyapunov exponent fluctuates about zero. *Phys. Rev. Lett.*, 73(14):1927–1930, 1994.

[7] R.L. Viana, J.R.R. Barbosa, and C. Grebogi. Unstable dimension variability and codimension-one bifurcations of two-dimensional maps. *Phys. Lett. A*, 321:244–251,

2004.

[8] Y.-C. Lai and C. Grebogi. Modeling of coupled chaotic oscillators. *Phys. Rev. Lett.*, 82(24):4803–4806, 1999.

[9] Y. Do and Y.-C. Lai. Statistics of shadowing time in nonhyperbolic chaotic systems with unstable dimension variability. *Phys. Rev. E*, 69:016213, 2004.

[10] C. Bonatti, L.J. Díaz, and M. Viana. *Dynamics Beyond Uniform Hyperbolicity.* Springer, New York, 2005.

[11] W. Zhang, B. Krauskopf, and V. Kirk. How to find a codimension-one heteroclinic cycle between two periodic orbits. *Discrete Contin. Dyn. Syst.*, 32(8):2825–2851, 2012.

[12] A. Hammerlindl, B. Krauskopf, G. Mason, and H.M. Osinga. Determining the global manifold structure of a continuous-time heterodimensional cycle. To appear: *J. Comput. Dyn.*, 2022.

[13] Ch. Bonatti, S. Crovisier, L.J. Díaz, and A. Wilkinson. What is... a blender? *Notices AMS*, 63(10):1175–1178, 2016.

[14] A. Avila, S. Crovisier, and A. Wilkinson. c^1 density of stable ergodicity. *Adv. Math.*, 379:107496, 2021.

[15] C. Bonatti and L.J. Díaz. Robust heterodimensional cycles and C^1-generic dynamics. *J. Inst. Math. Jussieu*, 7:469–525, 2008.

[16] C. Bonatti, L.J. Díaz, and S. Kiriki. Stabilization of heterodimensional cycles. *Nonlinearity*, 25:931–960, 2012.

[17] S. Hittmeyer, B. Krauskopf, H.M. Osinga, and K. Shinohara. Existence of blenders in a Hénon-like family: geometric insights from invariant manifold computations. *Nonlinearity*, 31(10):R239–R267, 2018.

[18] S. Hittmeyer, B. Krauskopf, H.M. Osinga, and K. Shinohara. How to identify a hyperbolic set as a blender. *Discrete Cont. Dyn. Syst.*, 40(12):6815–6836, 2020.

[19] Y. Saiki, H. Takahasi, and J.A. Yorke. Piecewise-linear maps with heterogeneous chaos. *Nonlinearity*, 34:5744–5761, 2021.

[20] A.S. Gonchenko, S.V. Gonchenko, A.O. Kazakov, and A.D. Kozlov. Elements of contemporary theory of dynamical chaos: A tutorial. Part I. Pseudohyperbolic attractors. *Int. J. Bifurcation Chaos*, 28(11):1830036, 2018.

[21] S. Gonchenko, A. Kazakov, and D. Turaev. Wild pseudohyperbolic attractor in a four-dimensional Lorenz system. *Nonlinearity*, 34:2018–2047, 2021.

[22] S.V. Gonchenko, I.I. Ovsyannikov, C. Simó, and D. Turaev. Three-dimensional Hénon-like maps and wild Lorenz-like attractors. *Int. J. Bifurcation Chaos*, 15(11):3493–3508, 2005.

[23] P. Glendinning. Heterodimensional cycles and noninvertible blenders in piecewise smooth two dimensional maps. *https://arxiv.org/abs/2304.05689*, 2023.

[24] Z.T. Zhusubaliyev, O.O. Yanochkina, E. Mosekilde, and S. Banerjee. Two-mode dynamics in pulse-modulated control systems. *Annual Rev. Control*, 34:62–70, 2010.

[25] M. di Bernardo, P. Kowalczyk, and A. Nordmark. Sliding bifurcations: A novel mechanism for the sudden onset of chaos in dry friction oscillators. *Int. J. Bifurcation Chaos*, 13(10):2935–2948, 2003.

[26] R. Szalai and H.M. Osinga. Arnol'd tongues arising from a grazing-sliding bifurcation. *SIAM J. Appl. Dyn. Sys.*, 8(4):1434–1461, 2009.

[27] T. Puu and I. Sushko, editors. *Business Cycle Dynamics: Models and Tools.* Springer-Verlag, New York, 2006.

[28] D.J.W. Simpson. Border-collision bifurcations in $\mathbb{R}^n$. *SIAM Rev.*, 58(2):177–226, 2016.

[29] H.E. Nusse and J.A. Yorke. Border-collision bifurcations including "period two to period three" for piecewise smooth systems. *Phys. D*, 57:39–57, 1992.

[30] M. di Bernardo. Normal forms of border collision in high dimensional non-smooth maps. In *Proceedings IEEE IS-CAS, Bangkok, Thailand*, volume 3, pages 76–79, 2003.

[31] S. Banerjee and C. Grebogi. Border collision bifurcations in two-dimensional piecewise smooth maps. *Phys. Rev. E*, 59(4):4052–4061, 1999.

[32] D.J.W. Simpson and J.D. Meiss. Neimark-Sacker bifurcations in planar, piecewise-smooth, continuous maps. *SIAM J. Appl. Dyn. Sys.*, 7(3):795–824, 2008.

[33] P. Glendinning and D.J.W. Simpson. Chaos in the border-collision normal form: A computer-assisted proof using induced maps and invariant expanding cones. *Appl. Math. Comput.*, 434:127357, 2022.

[34] S. Banerjee, J.A. Yorke, and C. Grebogi. Robust chaos. *Phys. Rev. Lett.*, 80(14):3049–3052, 1998.

[35] I. Ghosh and D.J.W. Simpson. Robust Devaney chaos in the two-dimensional border-collision normal form. *Chaos*, 32:043120, 2022.

[36] M. Misiurewicz. Strange attractors for the Lozi mappings. In R.G. Helleman, editor, *Nonlinear dynamics, Annals of the New York Academy of Sciences*, pages 348–358, New York, 1980. Wiley.

[37] D.J.W. Simpson and P.A. Glendinning. Inclusion of higher-order terms in the border-collision normal form: persistence of chaos and applications to power converters. Submitted to: *Phys. D.* `arXiv:2111.12222`, 2021.

[38] D.J.W. Simpson. Unfolding homoclinic connections formed by corner intersections in piecewise-smooth maps. *Chaos*, 26:073105, 2016.

[39] P.A. Glendinning and D.J.W. Simpson. A constructive approach to robust chaos using invariant manifolds and expanding cones. *Discrete Contin. Dyn. Syst.*, 41(7):3367–3387, 2021.

[40] P. Glendinning and C.H. Wong. Two dimensional attractors in the border collision normal form. *Nonlinearity*, 24:995–1010, 2011.

[41] P. Glendinning. Bifurcation from stable fixed point to 2D attractor in the border collision normal form. *IMA J. Appl. Math.*, 81(4):699–710, 2016.

[42] J.-P. Eckmann and D. Ruelle. Ergodic theory of chaos and strange attractors. *Rev. Mod. Phys.*, 57(3):617–656, 1985.

[43] H.F. von Bremen, F.E. Udwadia, and W. Proskurowski. An efficient QR based method for the computation of Lyapunov exponents. *Phys. D*, 101:1–16, 1997.

[44] J.-P. Duval. Génération d'une section des classes de conjugaison et arbre des mots de Lyndon de longueur bornée. *Theoret. Comput. Sci.*, 60:255–283, 1988. In French.

[45] J. Berstel and M. Pocchiola. Average cost of Duval's algorithm for generating Lyndon words. *Theoret. Comput. Sci.*, 132:415–425, 1994.

[46] P. Glendinning. Bifurcations of snap-back repellers with application to border-collision bifurcations. *Int. J. Bifurcation Chaos*, 20:479–489, 2010.

[47] S. De, P.S. Dutta, S. Banerjee, and A.R. Roy. Local and global bifurcations in three-dimensional, continuous, piecewise-smooth maps. *Int. J. Bifurcation Chaos*, 21(6):1617–1636, 2011.

[48] D.J.W. Simpson. Grazing-sliding bifurcations creating infinitely many attractors. *Int. J. Bifurcation Chaos*, 27(12):1730042, 2017.

[49] K.T. Alligood, E. Sander, and J.A. Yorke. Crossing bifurcations and unstable dimension variability. *Phys. Rev. Lett.*, 96:244103, 2006.

[50] E. Barreto and P. So. Mechanisms for the development of unstable dimension variability and the breakdown of shadowing in coupled chaotic systems. *Phys. Rev. Lett.*, 85(12):2490–2493, 2000.